Desalination and Water Treatment
www.deswater.com

doi:10.5004/dwt.2016.0246

66 (2017) 149–157
March

Utilization of seafood processing waste as an adsorbent in the treatment of paint industry effluent in a fixed-bed column

Solaiappan Vishali[a,*], Ramasamy Karthikeyan[b], Sivaraman Prabhakar[a]

[a]*Department of Chemical Engineering, SRM University, Kattankulathur, Chennai, Tamil Nadu, India – 603 203, Tel. +91-9443883562, email: meet.vishali@gmail.com (S. Vishali), Tel. +91-9445259977, email: sivaprabha50@gmail.com (S. Prabhakar)*
[b]*Anjalaiammal Mahalingham Engineering College, Thanjavur, Tamil Nadu, India – 614 403, Tel. +91-9940561915, email: drrkarthi@yahoo.com (R. Karthikey)*

Received 3 March 2016; Accepted 22 June 2016

ABSTRACT

The potentiality of seafood processing waste *P. sanguinolentus* (crab shell) as an adsorbent was assessed in fixed bed absorption (FBC) column for the treatment of paint industry effluent (PIE). The effect of bed height (10–25 cm), flow rate (5–15 cc/min) and initial concentration (3100–7693 mg/L) were studied with reference to the colour removal efficiency. Breakthrough curves were generated and based on the data the extent of suitability of different models was studied to identify limiting mechanism of the adsorption process. It was concluded that the intra particle diffusion was not the only rate controlling step, but film diffusion was also a likely influencing factor. The studies further indicated that *P. sanguinolentus* (crab) shell could be effectively used for PIE treatment

Keywords: Adsorption; Crab shells; Paint industry effluent; Mass transfer; Fixed-bed; Break through curve

1. Introduction

In the generated wastewater from paint industry effluent (PIE), 80% is from cleaning of mixers, reactors, blenders, packing machines and floors [1] and not from the manufacturing process itself. Effluents from the paint industry contain highly toxic and organic bio-refractory compounds accounting for COD, BOD and TOC, which endanger aquatic life and wildlife and contaminate the food chain. The direct release of this effluent into the surrounding aquatic environment poses serious health risks, resulting in toxicity to both human and aquatic life by the accumulation of toxic compounds in the environment. It can also contribute to respiratory disorders, irritation of eyes, skin, lungs, cause headache, muscle weakness and damage to liver and kidney. Legal restrictions in organized industrial zones make it mandatory for the effluent to be treated suitably before being discharged into the environment, in this way promoting environmental conservation [2].

*Corresponding author.

Various traditional techniques are available for the removal of pollutant from PIE. It was effectively treated using the plant-based materials *S. potatorum* and *C. opuntia* as a natural coagulant [3,4]. When weighing the traditional techniques against each other, it was found that the adsorption process was more economical, efficient and simple. Activated carbon adsorption has been proved to be the most popular and effective method for the removal of color and heavy metals from water and wastewater.

The large surface area, high porosity, considerable amount of mechanical strength and high degree of surface reactivity make activated carbon an ideal adsorbent, but the cost factor imposes restrictions on its application in the paint industry. The preparation of new and effective low-cost adsorbent is extremely essential for the treatment of paint effluent [5]. Researchers today focus mainly on achieving maximum removal of pollutant ions by the use of low-cost and plentifully available materials. Successful treatment of wastewater not only depends on the pollutant removal ability of the adsorbent, but also requires an abundance of the material for the purpose. It follows therefore that the adsorbent should either be an industrial waste product or one

that is Available plenty in nature [6]. Crab shell were exhibited its coagulant properties effectively in the treatment of PIE [7]. An attempt has been made in the present study to use the, crab shell, universally available, seafood processing waste as an adsorbent in the treatment of PIE.

2. Materials and methods

2.1. Materials

2.1.1. Chemicals

All chemicals used in the study were of analytical grade (AR). They were procured from Merck India.

2.1.2. Effluent

The effluent, named as simulated water based paint industry effluent (PIE), was prepared whenever it was required, by adding different proportions of commercially available white primer and an acrylic based blue colorant, which was then made up to 1000 mL using double distilled water (5% v/v). Paint volume was measured using a syringe. Three samples with different initial concentration were prepared and labeled as Sample numbers 1, 2 and 3, respectively (Table 1). The physico-chemical characteristics of the effluent were analyzed and the results are given in Table 2 [8].

2.1.3. Adsorbent

P. sanguinolentus (crab) shells sourced from Jegathapattinam situated on the eastern coast were purchased from the local sea food market of Pudukottai, South India. The shells of three rod spotted crab were washed thoroughly with deionized water to remove the soft tissues within, sun dried for 2 h, crushed using a standard kitchen blender and the powder sieved through a 0.5 mm sieve (Fig. 1).

Table 1
Concentration of simulated PIE (made upto 1000 mL)

Sample number	White primer (mL)	Blue colorant (mL)	Initial COD (mg/L)
1	48	2	3100
2	44	6	5650
3	40	10	7693

Table 2
Physico-chemical characteristics of the simulated PIE (Sample number 3)

Parameters	Concentration (except for pH, color and turbidity)
pH at 25°C	7.6
Color	Blue
Total dissolved solids, mg/L	304
Total suspended solids, mg/L	6880
Oil and grease, mg/L	19
Chloride as Cl, mg/L	68
Chemical oxygen demand (COD), mg/L	7693
Sulfate as SO_4, mg/L	24
Biochemical oxygen demand, mg/L	
(3 days incubated at 27°C)	2648
Iron as Fe, mg/L	0.05
Turbidity, NTU	7760

2.1.4. A fixed bed column

A fixed bed column (FBC) made up of Pyrex glass with an inner diameter 2 cm and length 50 cm with tapered end was fabricated for lab facility, to conduct the continuous adsorption process. The effluent was introduced into a FBC, using a peristaltic pump (Ravel Hitek, India) at a room temperature 30ºC.

2.2. Methods

2.2.1. Preparation of immobilized beads

For immobilization of adsorbent *P. sanguinolentus*, sodium alginate was used as a matrix. The powdered material (3 % (w/v)) and sodium alginate (1 % (w/v)) was suspended in distilled water. This suspension was done using magnetic stirrer with hot plate. The temperature was main-

Fig. 1. *P. sanguinolentus* (crab) shells, powder and immobilized beads.

tained as not more than 45 ºC, in order to avoid the loss of adsorption properties of the adsorbent. The resultant slurry was extruded as a drop in sterile 3% $CaCl_2$ solution at room temperature, using syringe. The beads were hardened by re-suspending in a fresh $CaCl_2$ solution for 24 h at 4ºC and finally these beads were washed with de-ionised water to remove excess calcium ions. Immobilized beads without the addition of natural materials were used as a control [9].

2.2.2. Adsorption experiments

Fixed bed column (FBC) studies were carried out using a Pyrex glass column of 2 cm internal diameter and 50 cm length. The column was placed with glass wool in the bottom. Immobilized beads made from natural material were packed in the column to the desired height, between two supporting layers of glass beads. The presence of glass wool at the bottom was to avoid the blockage of glass beads in the outlet. The adsorbate was introduced in a down flow mode, using a peristaltic pump at a room temperature of 30ºC without any pH adjustment.

Uniform packing of the adsorbent (because of terminal settling velocity) was ensured for every run by filling the column with de-ionized water, after which the beads were slowly added. When the desired height of the column is attained the water was drained to ensure compact packing. Prior to every run, the mass of the adsorbent used in the packing was noted. The treated effluent samples were collected at specific time intervals and analyzed for residual color. The column studies were concluded when the column reached exhaustion point. All the experiments were carried out at least thrice to ensure reproducibility. The reported values were the average of three data sets. A series of experiments were carried out to study the effect of flow rate, bed height and initial concentration of effluent. The effect of operating variables on a FBC design parameters are listed in Table 3.

2.2.3. Performance analysis

The treatment efficiency was assessed in terms of removal of color, using SL 218 double

UV visible spectrophotometer (Elico – India) at λ_{max} 612 nm.

3. Results and discussion

3.1. Characterization of P. sanguinolentus (crab) shells

The characterizations of *P. sanguinolentus* (crab) shell was done using Fourier transform infrared spectroscopy (FTIR), Energy-dispersive X-ray spectroscopy (EDS), Scanning electron microscope (SEM) and X-ray diffraction (XRD).

Chitin is the most important natural polysaccharide found in cretaceous shells or in the cell walls of fungi. Its principal derivative is Chitosan obtained by deacetylation of chitin. Due to the presence of amino group it is soluble in aqueous acidic medium [10]. The samples of Chitosan produced (in KBr pellets) were characterized by using an infrared spectrophotometer in the range of 400–4000 cm^{-1} (ABB MB 3000) [11].

In general, chitosan from *P. sanguinolentus* shows bands at 3000–3500 cm^{-1} (NH bond) and at 1400–1650 cm^{-1} (C=O bond). The spectra of chitosan showed a broad absorption band in the range 3000 cm^{-1}–3500 cm^{-1} attributed to O–H stretching vibrations (Fig. 2a). The peaks around 2885, 1650, 1589, 1326 and 1080 cm^{-1} in the FT-IR spectrum of chitosan are due to the stretching vibrations of aliphatic C– H, Amide I (–NH deformation of $–NHCOCH_3$), Amide II, Amide III and C–O–C, bonds, respectively [12]. The FTIR spectrum of the *P. sanguinolentus* was obtained and the effective peaks were compared with that of the standard chitin and standard chitosan (Table 4a, b) and the presence of chitosan was confirmed. The elemental analysis of crab shells using Energy-dispersive X-ray spectroscopy (EDS), the scanning electron microscope (SEM) image and the X-ray Diffraction (XRD) image are given in Fig. 2b–d, respectively.

3.1.1. Characterization of immobilized P. sanguinolentus (crab) shell beads

The mean diameter (d) of the immobilized bead was calculated as, 0.5347 cm, using volume displacement method. By measuring the weight of known number of beads and its diameter, bead density was calculated. The bulk density (ρB) of the adsorbent was calculated as, 0.9554 g/mL, using the ratio between the total mass of the beads used for the required packing height per volume of the beads. The average bed porosity was 0.5211 and the apparent density of the bead (ρP) was noticed as 0.8775 g/mL

3.2. Effect of operating variables on breakthrough curves

3.2.1. Effect of bed height on breakthrough curves

Bed height becomes important when designing an adsorption column to treat specific loads of pollutant in an effluent and inadequate bed height would result in poor adsorption behavior. It relates the number of active sites available for adsorption. To demonstrate the effect of bed height with the help of an experimental breakthrough curve (Fig. 3a), this parameter was varied between 10 and 25 cm, while maintaining flow rate (5 cc/min) and initial concentration (3100 mg/L) of effluent as constant, without altering the initial pH.

The total time, corresponding to the stoichiometric capacity of the column, was found to be enhanced with a rise in the bed height from 10 to 25 cm (Table 3). The shape of the breakthrough curve depends on the bed height and therefore mass of adsorbent. The consistent increase in volume of the aqueous solution with increase in bed height was due to the availability of more number of sorption sites. This means that the greater the bed height, the more the mass of adsorbent and the better its capacity for adsorbing color from PIE [13].

3.2.2. Effect of flow rate on breakthrough curves

The flow rate of PIE stream determines the contact time between effluent and adsorbent. In the present study, the flow rate was varied as 5, 10 and 15 cc/min with controlled bed height and initial concentration.

The uptake of pollutant (color) was maximum in the initial stages, reduced gradually and finally reached satu-

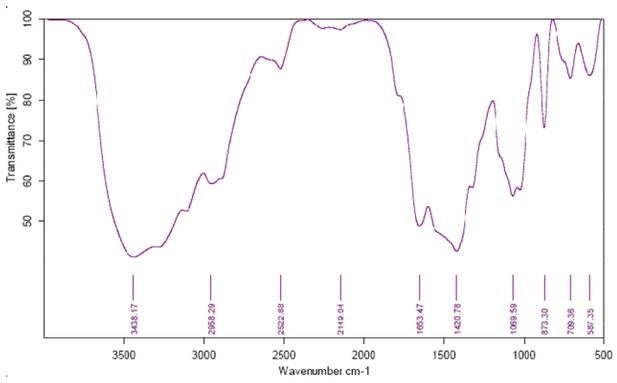

Fig. 2a. Fourier transform infrared spectroscopy (FTIR) spectrum of *P.sanguinolentus*

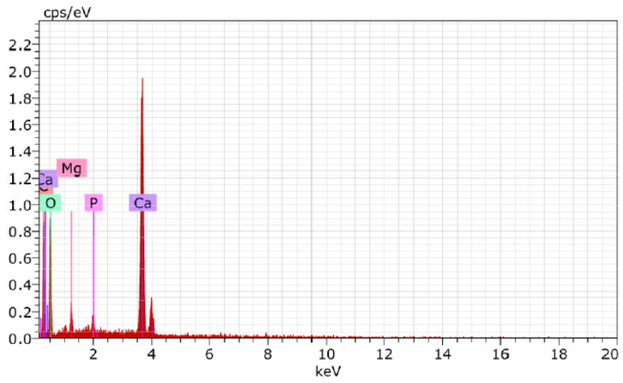

Fig. 2b. Elemental analysis of *P.sanguinolentus* using Energy-dispersive X-ray spectroscopy (EDS)

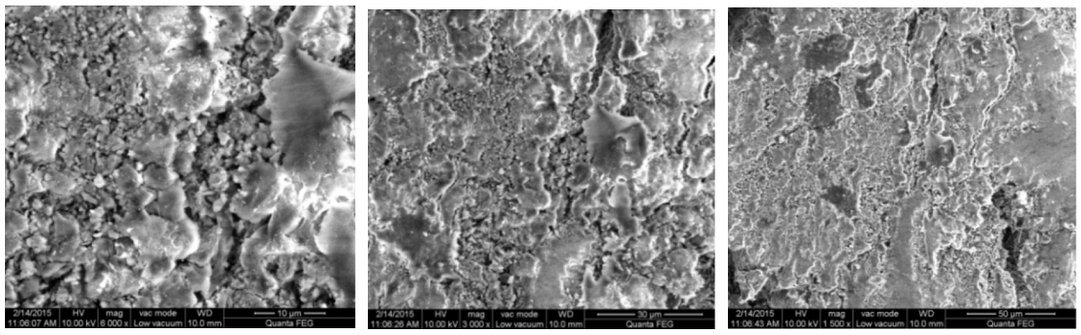

Fig. 2c. Scanning electron microscope (SEM) image of *P.sanguinolentus*

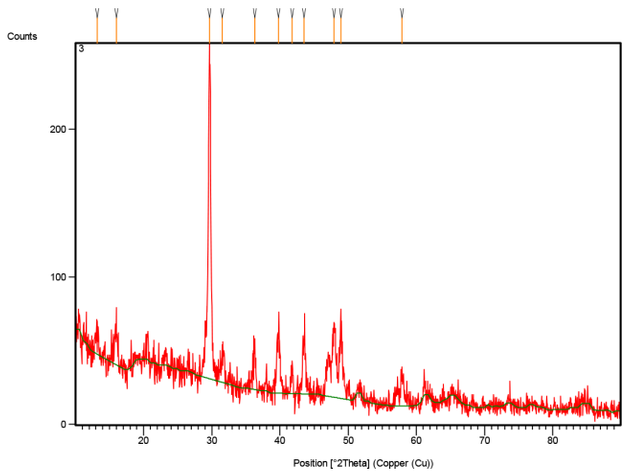

Fig. 2d. X-ray diffraction (XRD) of P.sanguinolentus

ration point (Fig. 3b). Lowering of the flow rate prolonged contact time but narrowed down the adsorption zone. When the volumetric flow rate reduced from 15 to 5 cc/min exchange mechanism (akin to ion exchange conditions) was more favorable. In contrast the breakthrough curves became steeper and reached the breakthrough point in a shorter period when flow rates were increased. This may be attributed to the fixed saturation capacity of the bed irrespective of the differences in concentration not withstanding the high flow rate. It was possible to attain adsorption equilibrium due to the length of the column. The contact time between pollutant and adsorbent was very brief at higher flow rates, resulting in a fall of removal efficiency (Table 3) [13].

3.2.3. Effect of initial effluent concentration on breakthrough curves

The effect of initial effluent concentration on the breakthrough curves at bed height of 25 cm and flow rate of 5 cc/min is shown in Fig. 3c. According to Fig. 3c, as the initial effluent concentration rose from 3100 to 7693 mg/L, the following parameters showed a downward trend: breakthrough time (from 333 to 171 min), total time corresponding to stoichiometric capacity of the column (from 350 to 180 min), volume of treated water (1750, 1150 and 900 mL), total percentage removal of color for a FBC (93%, 79% and 66%) (Table 3).

Increase in the initial concentration resulted in early saturation as expected bringing about faster appearance of the break point. It was observed that at higher initial concentration of adsorbate, adsorption sites became saturated rapidly, leading to a shorter breakthrough time. Conversely breakthrough was delayed for a lower adsorbate concentration and adsorbent surface took a longer time to get saturated [14].

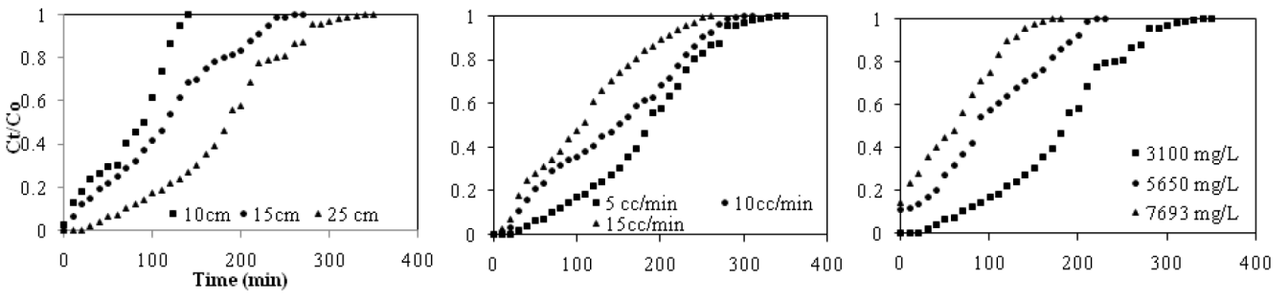

Fig. 3. Influence of operating variables on breakthrough curves in a FBC.
(a) Bed height (b) Flow rate (c) Initial concentration
(a) Bed height: 10–25 cm; Flow rate: 5 cc/min; Initial conc.: 7693 mg/L
(b) Bed height: 25 cm; Flow rate: 5-15 cc/min; Initial conc.: 7693 mg/L
(c) Bed height: 25 cm; Flow rate: 5cc/min; Initial conc.: 3100–7693 mg/L

Table 3
Influence of operating variables on a FBC design parameters

Co mg/L	Q cc/min	H cm	t_t min	q_t mg/g	t_b min	t_s min	V_{eff} mL	EBRT min	Total color removal %	MTZ cm
3100	5	10	150	28	143	7.5	750	6.28	86	9.47
3100	5	15	250	65	238	12.5	1250	9.42	90	14.21
3100	5	25	350	71	333	17.5	1750	15.7	93	23.68
3100	10	25	320	73	304	16	3200	7.9	52	23.68
3100	15	25	270	67	257	13.5	4050	5.2	38	23.68
5650	5	25	230	108	219	11.5	1150	15.7	79	23.68
7693	5	25	180	178	171	9	900	15.7	66	23.68

3.3. Modeling of breakthrough curves

Prediction of the breakthrough curve for an effluent is essential to enable successful design of an efficient adsorption column process with immobilized beads as an adsorbent. As such, it is necessary to fit the experimental adsorption data using established models and subsequently determine the relevant parameters to understand their effect on optimization of the fixed bed adsorption process [15].

3.3.1. Thomas or Bed depth service time (BDST) model

From the slope and intercept of the linear Thomas model (ln (C_t / (C_o – C_t)) vs. time), it was demonstrated that the model rate constant k_{BDST} and the adsorption capacity q_{BDST} were dependent on flow rate, bed height and initial concentration of adsorbate. A high regression coefficient (R^2) value indicated that the kinetic data conformed well to the Thomas model (Table 4).

The linearized form of Thomas model in with different bed-heights, flow rates and initial concentrations clearly indicate good agreement of the experimental data with the theoretically calculated values. The maximum adsorption capacity q_0 showed an increase with higher flow rates and higher initial concentration, but decreased with the increase in the bed height. It is understandable as the driving force behind for the adsorption is concentration gradient. Consequently maximum q_0 value was observed at higher initial concentration and higher flow rates [16].

The kinetic constant k_{TH} increased with flow rate but showed a decreasing trend with increasing bed height and initial concentration. This stemmed from the unavailability of reaction sites for the facilitation of the adsorption process. The step-up of k_{Th} value led to the interpretation that lower flow rate, low concentration and higher bed heights would increase efficiency of adsorption. Concurrence of the experimental data with the Thomas model indicated that neither external nor internal diffusion would be the limiting step [17].

3.3.2. Adams-Bohart model

The adsorbent displayed a gradual downward slant in their adsorption capacity with augmented flow rate of effluent (Table 5). The presence of more number of saturation sites, combined with shorter contact time between the adsorbent and adsorbate, led to a reduction in adsorption capacity of the adsorbent N_0 when flow rate was raised. A combination of lower flow rate, low concentration and higher bed heights would improve adsorption. The elevated initial concentration enhanced the maximum adsorption capacity per unit volume of adsorption column or N_0 (mg/L). The driving force behind adsorption was the concentration difference between the pollutant on the surface of the adsorbent and in the effluent. The concentration gradient increased with initial concentration [18].

Table 4a
Wavelength of the main bands obtained for the standard chitin and *P.sanguinolentus*

Vibration modes	Standard-α-chitin (cm^{-1})[130]	*P. sanguinolentus*-α-chitin (cm^{-1})
OH out of plane bending	690	709.36
NH out of plane bending	752	750
CH_3 wagging along chain	952	1000
CO stretching	1026	1024
CO stretching	1073	1069
CH_2 bending and CH_3 deformation	1418	1420
Amide I band	1661	1663
CH stretching	2878	2862
Symmetric CH_3 stretching and asymmetric CH_2 stretching	2930	2958
NH stretching	3268	3252
OH stretching	3439	3438.17

Table 4.b
Wavelength of the main bands obtained for the standard chitosan and *P. sanguinolentus*

Vibration modes	Standard-chitosan (cm^{-1}) [131]	*P. sanguinolentus* chitosan (cm^{-1})
HPO_4^{2-}	891.41	912
PO_4^{3-}	1026.63	1031
PO_3^4	1259.54	1249
OH group (monomer)	1422.73	1420.78
($-NH_2$) Amide II	1587.94	1575
Structural Unit	3377.95	3438.17

Table 5
Parameters of breakthrough models in a FBC at various conditions

				BDST		Adams-Bohart			Yoon-Nelson					Wang
C_o	Q	H	k_{BDST}	q_{BDST}	R^2	k_{AB}	N_0	R^2	k_{YN}	τ	R^2	k_W	$t_{0.5}$	R^2
mg/L	cc/min	cm	L/ (min. mg)	mg/g		L/(min. mg)	mg/L		1/min	min		1/min	min	
3100	5	10	0.0861	7.39	0.909	0.0450	9.33	0.823	0.0374	85	0.906	0.016	30	0.726
3100	5	15	0.0631	5.30	0.948	0.0205	9.41	0.765	0.0274	98	0.945	0.016	40	0.840
3100	5	25	0.0665	5.22	0.918	0.0288	7.89	0.774	0.0289	180	0.918	0.015	88	0.689
3100	10	25	0.0525	8.66	0.900	0.0214	14.7	0.710	0.0228	149	0.900	0.012	62	0.736
3100	15	25	0.0592	10.04	0.946	0.0223	18.2	0.717	0.0257	116	0.946	0.015	46	0.852
5650	5	25	0.0247	4.60	0.877	0.0085	32.8	0.875	0.0197	86	0.877	0.012	22	0.732
7693	5	25	0.0229	8.91	0.983	0.0082	52.5	0.885	0.0404	76	0.983	0.025	34	0.893

4.3.3. Yoon–Nelson model

A plot of ln $[C_t/(C_o - C_t)]$ versus t gave a straight line with slope of k_{YN} and intercept of τ. The values of k_{YN}, τ and adsorption capacity, q_o obtained are listed in Table 5. The time required for 50% breakthrough τ reduced with elevation of both flow rate and initial ion concentrations. High values of correlation coefficients indicated that the Yoon and Nelson model fitted well with the experimental data. It was also found that the rate constant (k_{YN}) increased in parallel with increase in flow rate. As a result of lowered residence time of pollutants in the adsorbent bed, the time required for 50% adsorbate breakthrough (τ) came down with a rise in flow rate. A larger residence time of adsorbate within the column caused the τ value to elapse with a

rise in the bed height. As is evident, the experimental data was compliant with the model. It can be concluded that Yoon-Nelson model is an appropriate model to describe fixed-bed operations [18].

4.3.4. Wang model

Wang model is a mass transfer model used to describe the breakthrough curve of solutions containing pollutants in the fixed bed. A plot of ln $[1/(1 - (C_t/C_o)]$ vs. t produces the slope and intercept value as $1/kw$ and $t_{0.5}$, respectively, where kw is the kinetic constant and $t_{0.5}$, time required for 50% adsorbate breakthrough time (min) (Table 5).

The time required for 50% breakthrough $t_{0.5}$, shortened with both faster flow rate and intensified initial ion concentration. The reason for such behavior was that slower flow rate ensured longer contact time with a resultant higher breakthrough time. The large amount of pollutant in terms of initial concentration took much time, to decolorize and reach 50% of its original quantity. The larger residence time of adsorbate within the column caused the $t_{0.5}$ value to elapse with a greater bed height. When immobilized *P. sanguinolentus* (crab) shells were used as an adsorbent, there was no noteworthy difference in kw values with respect to bed height or flow rate. This was due to the facts that increase in initial amount of the colour in the PIE induced competition among the adsorbate molecules for occupying adsorption sites, thereby resulting in improved uptake rate. The rate constant increased along with initial concentration [19].

4.4. Mass transfer studies in a fixed bed column (FBC)

To identify and establish the rate-limiting steps of the overall adsorption process, the following models were analyzed: Weber and Morris model, Boyd model, Urano-Tachkawa model and Mathews-Weber model.

4.4.1. Weber-Morris model

The kinetic rate constant of Weber-Morris model took a downturn with a rise in bed height (0.2667, 0.2593 and 0.091). It rose (0.091, 0.1847 and 0.2459) parallel to the flow rate. The values became lower (0.091, 0.4857 and 1.234) with a rise in initial concentration. It can be seen from the small value of the intra-particle diffusion constant that the boundary layer has less significant effect on the diffusion mechanism of pollutant uptake by the adsorbent [20].

During the process of adsorption, in addition to being adsorbed onto the surface of the adsorbent, mass transfer may also take place due to intra particle diffusion. In such a situation, the plot will not pass through the origin, indicating that intra particle diffusion was not the singular rate-controlling step and that film diffusion should not be ruled out as a possible rate controlling factor. In the present study, large k_{WM} values pointed to easier diffusion and transport into the pores of the adsorbents. The value of intercept I gave an idea about the boundary layer thickness: the larger the intercept the greater is the boundary layer effect. The observed large intercept also indicated that the effects on mass transfer resistance on the adsorbate were gradually higher, Thereby suggesting that external mass transfer resistance could not be ignored (Table 6).

4.4.2. Boyd model

To demonstrate the slow steps involved in the adsorption process, the kinetics data was also subjected to Boyd kinetics model analysis. The plot of Bt against time showed that the points were scattered and did not pass through the origin. Effective diffusion coefficient was found to be higher, showing readings of 4.35 to 5.8 x 10^{-05} with flow rate and initial concentration. Mixed results were observed with increase in bed height as4.35 to 10.2 x 10^{-05} with10^{-05}, 7.61 x 10^{-05} and 4.35 x 10^{-05}(cm^2/s) (Table 6).

It can be hypothesized that the decolorization of PIE was mainly governed by the external mass transport where intra-particle diffusion was the rate-limiting step [21]. The presence of an intercept showed that diffusion was not the only observed mechanism of transfer. A linear plot, with its slope equal to B, would mean that pore diffusion is the rate-controlling step [22].

4.4.3. Urano-Tachkawa model

The constant of the internal diffusion was determined from the slopes of the lines of $f(q_t/q_e)$ on t and listed in Table 6b. The values were elevated with flow rate graduating from 5 to 15 cc/min and with an increase in initial concentration from 3100 to 7693 mg/L, the values were increased [23].

Table 6
Parameters of mass transfer models in a FBC at various conditions

			Weber-Morris		Boyd		Urano-Tachkawa		Mathews-Weber
C_o	Q	H	k_{WM}	R^2	D_i	R^2	D_{UT}	R^2	k_{MW}
mg/L	cc/min	cm	mg/(min0.5.g)		cm^2/min		cm^2/min		cm/min
3100	5	10	0.2593	0.7251	4.57E-05	0.3860	5.17E-05	0.5003	1.88E-05
3100	5	15	0.2667	0.9042	7.61E-05	0.6233	7.34E-05	0.6228	3.32E-06
3100	5	25	0.1847	0.6717	4.35E-05	0.4920	4.33E-05	0.5376	2.61E-06
3100	10	25	0.091	0.8260	4.93E-05	0.4927	4.83E-05	0.5026	2.09E-06
3100	15	25	0.2459	0.8733	5.8E-05	0.6719	5.67E-05	0.7092	1.98E-06
5650	5	25	0.4857	0.9712	5.07E-05	0.6914	4.83E-05	0.7156	2.29E-06
7693	5	25	1.234	0.8114	10.2E-05	0.6408	9.84E-05	0.6762	3.13E-06

Earlier workers [24] in this field reported D_{UT} values in the range of 10^{-12}–10^{-13} cm²/s for intra particle diffusion to be the rate-limiting step for the adsorption of organic compounds. As per this postulation, the rate-limiting step appeared to be particle diffusion since the D_{UT} values were in the order of 10^{-12} cm²/s. The adsorption process could be best explained by the Urano-Tachikawa equation, indicating the controlling nature of intraparticle diffusion.

4.4.4. Mathews-Weber model

It was noticed (Table 6b) that the kinetic constant values were increased from 1.88 x 10^{-05} to 3.32 x 10^{-06} with bed height. The contracted value of 2.61–1.98 x 10^{-06} was recorded with increase in flow rate. Similarly, an upward slant from 2.29 x 10^{-06} to 3.13 x 10^{-06} was observed with initial concentration. The k_{MW} values decreased with increments in the initial dye concentrations, indicating that the external mass transfer rate is slower at higher initial dye concentration. The velocity of dye transport from liquid phase to solid phase decreased but the intra particle diffusion increased with increase in the initial dye concentrations [25].

5. Conclusions

Column studies for the decolourisation of PIE were carried out using sodium alginate immobilized with *P. sanguinolentus* (crab) shell beads in a FBC. The percentage color removal was found to rise with an increase in the bed height and fall with an increase in flow rate and initial concentration. The presence of a large number of actives sites (due to larger bed height), higher mass transfer gradient (due to higher initial concentration) and larger residence time (due to lower flow rate) resulted in a higher adsorption capacity. Breakthrough curves were fitted with the curves of Thomas/BDST model, Adams-Bohart model, Yoon-Nelson model and Wang model. From the mass transfer models it was observed that the intra particle diffusion was not the only rate-controlling step, but film diffusion was also a likely influencing factor. In summary, it may be stated that *P. sanguinolentus* (crab) shell could be effectively used for the treatment of PIE, by virtue of being biodegradable, it is safe to human health, inexpensive, abundantly available and, last but not the least, efficient in the removal of toxic pollutants from PIE. It was also viewed that, it could serve as propitious surrogate for chemical activated carbon.

Symbols

a	—	total interfacial area of particle (cm²)
C_o, C_e, C_t	—	concentration of the solute, at t = 0, at equilibrium and time 't' in the effluent (mg/L)
d	—	Mean diameter of immobilized beads (cm)
D_i	—	Effective diffusivity (cm²/min)
D_UT	—	Diffusion constant in Urano-Tachkawa model (cm²/min)
H	—	Bed height (cm)
I	—	Thickness of boundary layer (mg/g)
k_{AB}	—	Kinetic constant in the model Adams-Bohart (L/(min · mg))
k_{BDST}	—	Kinetic constant in the model BDST, (L/(min · mg))
k_{MW}	—	External mass transfer coefficient from Mathews-Weber model(cm/min)
k_W	—	Kinetic constant in the model Wang (1/min)
k_{WM}	—	Kinetic constant in the model Weber-Morris (mg/(min 0.5. g))
k_{YN}	—	Kinetic constant in the model Yoon-Nelson (1/min)
m	—	Total mass of adsorbent (g)
N_o	—	Maximum adsorption capacity per unit volume of adsorption column(mg/L)
Q	—	Inlet feed flow rate (mL/min)
q_{BDST}	—	Maximum adsorption capacity in BDST model (mg/g)
q_t, q_e	—	Total quantity of pollutant adsorbed at time 't' and at equilibrium (mg/g)
r	—	Mean radius of immobilized adsorbent beads (cm)
R^2	—	Correlation coefficient
T	—	Absolute temperature (K).
t,t_b,t_s,t_t	—	Time, breakthrough time, saturation time, total time taken in FBC(min)
$t_{0.5}$	—	Time required for 50% adsorbate breakthrough time (min)
U_o	—	Linear velocity of inlet effluent (cm/min)
V,V_{eff}	—	Volume of effluent, Volume of effluent treated (mL)
τ	—	Time required for 50% adsorbate breakthrough time in Yoon-Nelson model (min)

References

[1] B.K. Dey, M.A. Hashim, S. Hasan, B. Gupta, Microfiltration of water-based paint effluents, Adv. Environ. Res., 8 (2004) 455–466.
[2] A. Akyol, Treatment of paint manufacturing wastewater by electro coagulation, Desalination, 285(31) (2012) 91–99.
[3] S. Vishali, R. Karthikeyan, A comparative study of *Strychnos potatorum* and chemical coagulants in the treatment of paint and industrial effluents: An alternate solution, Sep. Sci. Technol., 49 (16) (2014) 2510–2517.
[4] S. Vishali, R. Karthikeyan, *Cactus opuntia (ficus-indica):* an eco-friendly alternative coagulant in the treatment of paint effluent, Desali. Water Treat., 56 (6) (2014)1489–1497.
[5] P. Senthil Kumar, R.V. Abhinaya, G.K. Lashmi, V. Arthi, R. Pavithra, V. Sathya Selvabala, D.S. Kirupha, S. Sivanesan, Adsorption of methylene blue dye from aqueous solution by agricultural waste: Equilibrium, thermodynamics, kinetics, mechanism and process design, Colloid. J., 73 (5) (2001) 651–661.
[6] R.M. Sudhir Dahiya, A.G. Tripathi, Hegde, Biosorption of lead and copper from aqueous solutions by pre-treated crab and arca shell biomass, Bioresour. Technol., 8(99) (2008) 179–187
[7] S. Vishali, P. Rashmi, R. Karthikeyan, Evaluation of wasted biomaterial, crab shells *(Portunus sanguinolentus*), as a coagulant, in paint effluent treatment, Desali. Water Treat., 57(28) (2016) 13157–13165
[8] B.K. Korbahti, A. Tanyolac, Electrochemical treatment of simulated industrial paint wastewater in a continuous tubular reactor, Chem. Eng. J., 148(2–3) (2009) 444–451.
[9] S. Vishali, P. Rashmi, R. Karthikeyan, Potential of environmental-friendly, agro-based material *Strychnos potatorum*, as an

adsorbent, in the treatment of paint industry effluent, Desal. Water Treat., 57 (2016) 18326–18337.
[10] J. Brugnerotto, F.M. Lizardi, W. Goycoolea, J.A. Monal, M.D. Ares, Rinaudo, An infrared investigation in relation with chitin and Chitosan characterization, J. Polym., 42 (2001) 3569–3580.
[11] C. Palpandi, S. Vairamani, S. Annaian, Extraction of chitin and chitosan from shell and operculum of mangrove gastropod Nertia (dostia) crepidularia Lamarck, Int. J. Med. Med. Sci., 1(5) (2009) 198–205.
[12] T.S. George, K.S. Guru, N.S. Vasanthi, K.P. Kannan, Extraction, purification and characterization of chitosan from endophytic fungi isolated from medicinal plants, World J. Sci. Technol., 1(4) (2011) 3–48.
[13] J.T. Nwabanne, P.K. Igbokwe, Adsorption of packed bed column for the removal of lead (II) using oil palm fibre, Int. J. Appl. Sci. Technol., 2(5) (2012) 106–115.
[14] A. Naghizadeh, S. Nasseri, A.H. Mahvi, R. Nabizadeh, R.R. Kalantary, A.Rashidi, Continuous adsorption of natural organic matters in a column packed with carbon nanotubes, J. Environ. Health Sci. & Eng., 11(14) (2013) 1–6.
[15] X. Lin, R. Li, Q. Wen, J. Wu, J. Fan, X. Jin, W. Qian, D. Liu, X. Chen, Y. Chen, J. Xie, J. Bai, H. Ying, Experimental and modeling studies on the sorption breakthrough behaviors of butanol from aqueous solution in affixed bed of KA-I resin, Biotechnol. Bioprocess Eng., 18 (2013) 223–233.
[16] Z. Xu, J.G. Cai, B.C. Pan, Mathematically modeling fixed-bed adsorption in aqueous systems, J. Zhejiang Univ. Sci. A, 14(3) (2013) 155–176.
[17] Z.Z. Chowdhury, S.M. Zain, A.K. Rashid, R.F. Rafique, K. Khalid, Breakthrough curve analysis for column dynamics sorption of Mn(II) ions from wastewater by using *Mangostan agarcinia* Peel-based granular activated carbon J. Chem., (2013) 1–8.
[18] Z. Saadi, R. Saadi, R. Fazaeli, Fixed-bed adsorption dynamics of Pb (II) adsorption from aqueous solution using nanostructured γ-alumina, J. Nanostructure. Chem., 3(48) (2013) 1–8.
[19] Y.H. Wang, S.H. Lin, R.S. Juang, Removal of heavy metal ions from aqueous solutions using various low-cost adsorbents, J. Hazard. Mater., 102(2–3) (2003) 291–302.
[20] A.O. Okewale, K.A. Babayemi, A.P. Olalekan, Adsorption isotherms and kinetics models of starchy adsorbents on uptake of water from ethanol – water systems, Int. J. App. Sci. Technol., 3(1) (2013) 35–42.
[21] A.O. Okewale, P.K. Igbokwe, J.O. Ogbuagu, Kinetics and isotherm studies of the adsorptive dehydration of ethanol-water system with biomass based materials, Int. J. Eng. Innov. Technol., 2(9) (2013) 36–42.
[22] I.E. Hristova, Comparison of different kinetic models for adsorption of heavy metals onto activated carbon from apricot stones, Bulg. Chem. Commun., 43 (2011) 370–377.
[23] S.V. Dimitrova, Removal of lead (II) from aqueous solutions by blast-furnace metallurgical slags, Indian J. Eng Mater. Sci., 5 (1998) 89–193.
[24] V.P. Vinod, T.S. Anirudhan, Adsorption behavior of basic dyes on the humic acid immobilized pillared clay, Water Air Soil Pollut., 150 (2003) 193–217.
[25] E.W. Bao, Y.H. Yong, X. Lei, P. Kang, Biosorption behavior of azo dye by inactive CMC immobilized Aspergillus fumigates beads, Bioresour. Technol., 99 (2008) 794–800.